

Finite Element Analysis of a Mock Satellite Based on Launch Vehicle Requirements

a project presented to
The Faculty of the Department of Aerospace Engineering
San José State University

in partial fulfillment of the requirements for the degree
Master of Science in Aerospace Engineering

by
Conlan Berger

December 2021

approved by
Dr. M. Chierichetti
Faculty Advisor

© 2021

Conlan Berger

ALL RIGHTS RESERVED

Abstract
**Finite Element Analysis of a Mock Satellite Based on Launch Vehicle
Requirements**

Conlan Berger

Spacecraft launchers are used to transport payload and crew to low earth orbit and geosynchronous transfer orbit. The payload is placed inside the fairing of a launcher. Different countries use different launchers, and each launcher provides different vibration and thermal requirements. The United States uses the Delta IV, Atlas V, Falcon 9, and the Falcon Heavy. Russia uses the Zenit launcher. Europe uses the Vega, and the Ariane 5 and China uses the CZ5. Each launcher has different vibrational, thermal, and dimensional requirements that the satellite must meet in order to safely launch it into space. The finite element analysis will model the given requirements on the satellite in order to determine the launcher that should be used. Satellites vary in shape and size and are never one in the same. Modeling the structural vibration and thermal requirements is important to protect the payload and the launcher.

Table of Contents

1.Introduction	7
1.1 Motivation	7
1.2 Literature Review	8
1.2.1 Launch Vehicle Structures	8
1.2.2 Material selection	10
1.2.3 Failures in Launch Vehicles	10
1.2.4 Payload Fairing Structure	11
1.2.5 Launcher Requirements	11
1.3 Project Objective	13
1.4 Methodology	13
2.Launcher Structural Requirements	14
2.1 United States Launch Vehicles	14
2.1.1 Falcon 9	14
2.1.2 Atlas V	15
2.1.3 Delta IV	16
2.2 Russia Launch Vehicle	16
2.2.1 Zenit	16
2.3 Europe Launch Vehicles	17
2.3.1 Vega	17
2.3.2 Ariane 5	18
2.4 China Launch Vehicle	19
2.4.1 Long March	19
3. Vibration Equations	21
3.1 SDOF with Moving Base	21
3.2 Sinusoidal Vibrational Load with Moving Base	22
3.3 Random Vibrational Loads	24
3.4 Shock Vibration Loads	25
3.5 Finite element analysis	27
4. Mesh and Sinusoidal Analysis	28
4.1 Geometry of Satellite	28
4.2 Modal Analysis and Mesh Verification	29
4.3 Sinusoidal vibration load	32

5. Shock and Random Vibration Analysis	35
5.1 Shock Vibration Analysis	35
5.2 Random Vibration Analysis	37
6. Conclusion	40
References	41

Figures

Figure 1.1: Launch vehicles and total payload limit in tons [3]	10
Figure 1.2: General subsystem breakdown of a launch vehicle [7]	11
Figure 1.3: Payload fairing system components [14]	13
Figure 1.4: General axial force of a rocket [18]	14
Figure 2.1: Frequency of payload as acceleration increases [21]	16
Figure 2.2: Acceleration g-force for each adapter with frequency measured [22]	17
Figure 2.3: Frequency response of different adapters and the g-force experienced [24]	19
Figure 2.4: Frequency of payload as shock g-force increases [25]	20
Figure 2.5: Shock response relative to acceleration [26]	21
Figure 2.6: Frequency of shock vibration against g-force acceleration [27]	22
Figure 3.1: Mass with moving base example [28]	23
Figure 3.2: Basic sinusoidal profile for a spacecraft structure [29]	25
Figure 3.3: Sinusoidal profile for example 3.2.1	26
Figure 3.4: Falcon 9 shock response from example 3.4.1	28
Figure 4.1: Isometric view of monoblock satellite	30
Figure 4.2: Side view (left) and top view (right)	30
Figure 4.3: Spring-mass system within satellite	31
Figure 4.4: Mode shapes 1-3	31
Figure 4.5: Mode shapes 4 (top left)-7(bottom)	32
Figure 4.6: Mode convergence for tetra and hexa mesh	33
Figure 4.7: Linear(left) and tetra quadratic mesh(right)	34
Figure 4.8: Sinusoidal response of monoblock satellite	35
Figure 4.9: Sinusoidal profile of monoblock satellite	35
Figure 4.10: Double amplitude of sinusoidal profile	36
Figure 5.1: Shock response from acceleration of monoblock satellite	37
Figure 5.2: SRS acceleration curve	38
Figure 5.3: Falcon 9/Heavy random vibration example [31].....	39
Figure 5.4: Random vibration at the top face of the satellite	40
Figure 5.5: Random vibration of mass-spring system	40

Tables

Table 1.1: Orbital vehicle production by country [1].....	9
Table 4.1: Natural frequency of each mode shape	32
Table 4.2: Mesh verification parameters	33
Table 5.1: Shock response data from acceleration profile	38
Table 5.2: Data of random vibration.....	41

1.Introduction

1.1 Motivation

The dawn of the space age was dominated by the United States and the Soviet Union. The race to the moon initiated a transitional period to interplanetary exploration. Furthermore, launch vehicles and spacecraft were developed to extend the reaches of Earth. The vehicles allowed payload and crew to be safely transported to low earth orbit. Since 2007 the market for launcher vehicles has grown with more countries becoming invested in them. Table 1.1 below shows the percent increase in orbital vehicles launched since 1990 by country. In 1990 there were eight countries who had orbital vehicles, today there are 12 countries.

Table 1.1: Orbital vehicle production by country [1]

Period	Country of Production	Share
1990 to 1998	US	39%
	Russia	32%
	France	13%
	Ukraine	9%
	China	5%
	Japan	2%
	Israel, India	< 1%
2007 to mid-2009	Russia	30%
	US	26%
	China	14%
	Ukraine	13%
	France	8%
	India	4%
	Japan	2%
	Iran, Israel,	
	North Korea, South Korea	< 1%

Launch vehicles are designed to be as light as possible to maximize their payload weight but a launch vehicle operates close to its breaking point during a launch. The vehicle undergoes the stresses associated with accelerating past the speed of sound and navigating through the atmosphere [2]. The structure of a launch vehicle is the most important part of a launch vehicle but the payload experiences additional vibrational, thermal, and acoustic stresses as well. The payload is the primary objective and can be challenging and requires a detailed finite element analysis. The finite element analysis will simulate the primary vibrations the payload experiences. Understanding the equations and requirements that drive a safe launch, and delivering the payload to its destination, is fundamental in continuing our reach in space exploration.

1.2 Literature Review

1.2.1 Launch Vehicle Structures

Spacecraft have changed substantially as a result of innovative technologies and mission design. Early spacecraft performed multiple duties and served as long range weapons as well as launch vehicles. Today, spacecraft serve individual purposes and optimize performance and safety for its desired task. Launch vehicles have become the centerpiece of space technology as interplanetary studies have become more feasible. A launch vehicle is defined as an airborne system that delivers a payload from the ground to suborbital, orbital or interplanetary space [1].

The vehicles range in size and payload capacity. Newer designs such as the SLS Block 1 can transport heavier payloads to low Earth orbit. Figure 1.1 below shows the evolution of launch vehicles and the total tons the vehicle can carry to low Earth orbit.

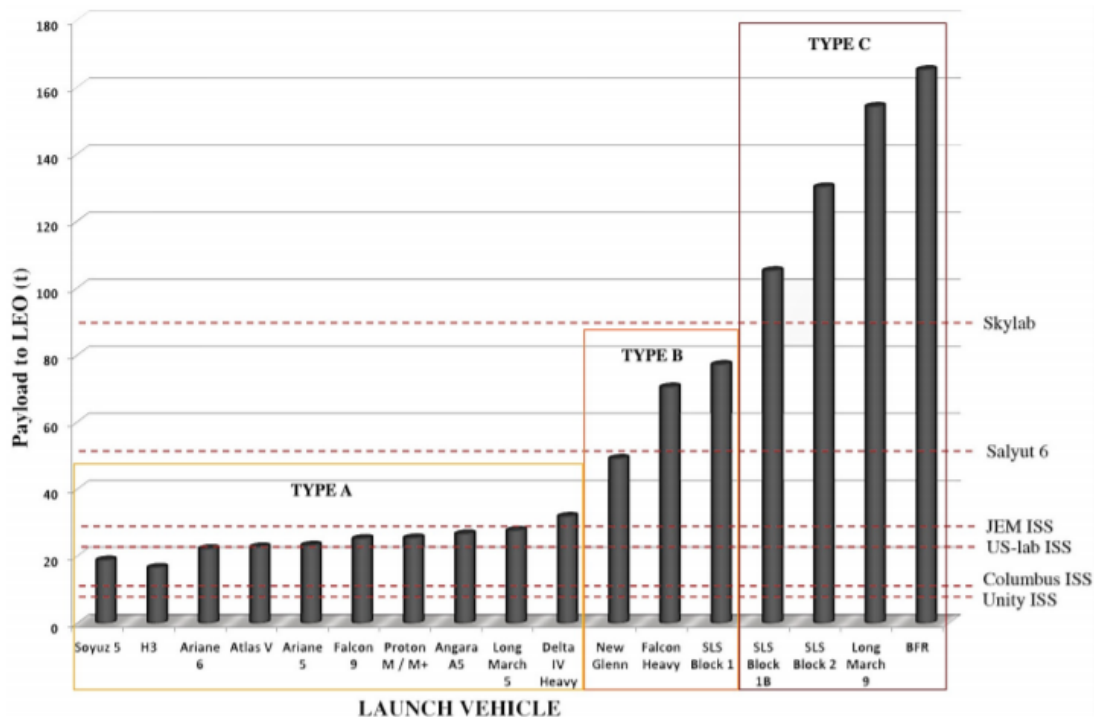


Figure 1.1: Launch vehicles and total payload limit in tons [3]

Launch vehicles contain a single stage or a two stage rocket propellant booster. The fairing is placed inside the forward end of the vehicle and the payload is stored in a shell attached to the upper stage rocket. A launch vehicle has similar subsystems compared to older spacecraft but the key differences are the operation time and velocity [4].

The structure of the launch vehicle is designed to protect the payload from bending and torsion, thermal exposure, and shock vibrations. The vehicle has numerous subsystems that rely on each other to safely launch and protect the payload. In general, the first stage of the launch vehicle is

designed from the engine up. The engine is designed to burn fuel and create gas that flows through the nozzle at supersonic speed and produces thrust of the rocket [5]. There are two primary fuel tanks that the engine draws from: a liquid fuel and an oxidizer. Most liquid fuel is a form of liquid hydrogen and the oxidizer is liquid oxygen. Liquid hydrogen mixed with liquid oxygen has the highest specific impulse to the amount of propellant consumed, of any known rocket propellant [6]. Upon separation of the first stage booster the second stage rocket propellant ignites and controls the payload fairing. The second stage contains the guidance and electrical system. The guidance system contains computers and radars coordinated with the rocket nozzle to perform directional maneuvers and provide stability for the payload fairing [7]. The guidance system stability function limits the bending and torsion the payload experiences, by keeping the second stage steady as it reaches low Earth orbit. Upon reaching low Earth orbit, the payload fairing shell will release and the third stage motor will ignite. The motor is designed to create thrust in space and deliver the payload into orbit or deliver it to its desired destination. The fairing shell separates because the payload is past any thermal and vibrational damages. Figure 1.2 below shows the general breakdown of all three stages of a launch vehicle. It shows the separation of each stage and the key components of each stage.

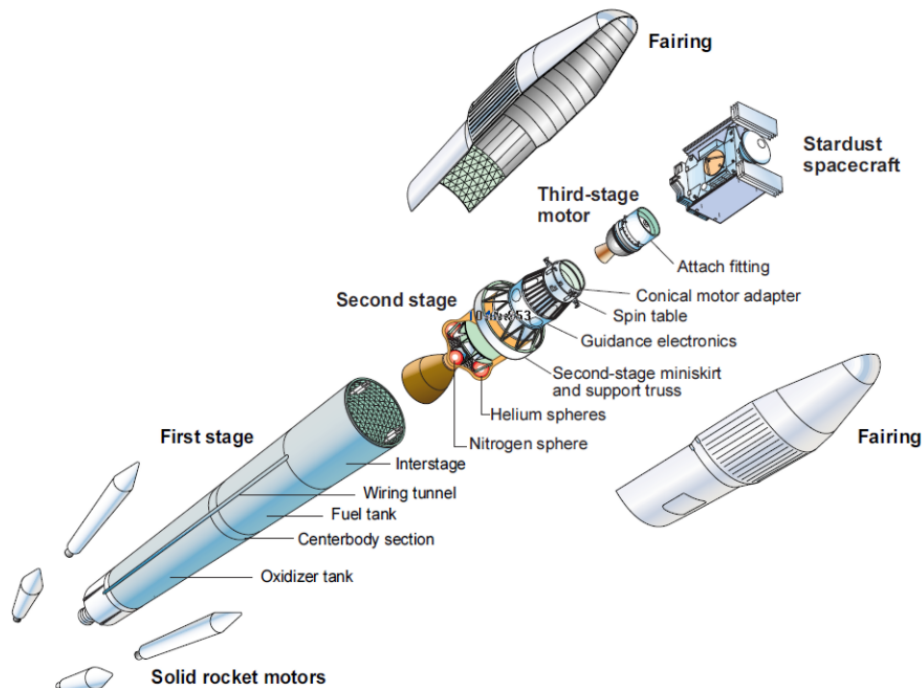


Figure 1.2: General subsystem breakdown of a launch vehicle [7]

The three stages of a launch vehicle are designed to deliver the payload to its designated orbit. The subsystems work alongside one another to limit stresses and thermal exposure to the payload. Each system is tested and analyzed before the use of it to ensure the protection of the payload.

1.2.2 Material selection

The material selection is one of the most important processes in the design of the structure. Most rocket frames use a duralumin series of aluminum alloys because of its high strength to weight ratio [8]. Duralumin aluminum alloys are susceptible to stress corrosion cracking based on the heat treatment used. However, it is still the most widely used material for rocket structures. It's the strongest of all aluminum alloys and comparable to steel, but weighs only a third of what steel weighs [9]. Aluminum alloys have been a fundamental component for newer rocket designs. Continuing, most modern rocket motors and booster bodies are made from forged steel [8]. The complex design of motors and boosters can be easily rolled from forged steel but won't lose any structural integrity or toughness. The payload fairing structure is further discussed in section 1.2.4. Overall, the structure of rockets are designed to be as strong as possible while limiting weight.

The use of liquid fuel and oxidizers have changed the material fuel tanks use. Liquid fuel tanks are made from titanium or aluminum alloys, and the interior lining must be a non-igniting layer [8]. Titanium is used with hydrazine fuel rockets and is high strength but much heavier than aluminum alloys. Aluminum is used for liquid hydrogen and liquid oxygen because of its non-reactive nature and high strength. Cryogenic fuels are stored at extremely low temperatures (< -300 degrees Fahrenheit) [10]. Aluminum is the best available material for storing cryogenic fuel for launch vehicles.

1.2.3 Failures in Launch Vehicles

Failures in launch vehicles are becoming less frequent as technology progresses but failure is in unison with learning. Therefore, launch vehicles will continue to fail for various reasons but problems can be solved because of it. The most common causes of failure are improper material selection and processing and a misuse of the components [11]. A study found that of all rockets launched until 2016, they had a failure rate of 8.9% [2]. This resulted in the loss or damage of over 400 satellites. The Challenger changed the way launchers and rockets were designed and tested. The O-ring failed due to the low temperature, which was due to the wrong material being used. Temperature at launch is one of the many failures that can occur during launch. Recently NASA found that the Taurus XL launch failures for the OCO and Glory missions were faulty aluminum used [12]. The payload fairing failed to separate on two occasions and the satellites were lost. Materials are the main reason for failures but recent developments have studied vibration isolators that launch vehicles and payloads use. They are used to protect electronic and guidance systems from the rigors of vibration during flight [13]. The isolators have been found to have substantial cracks and damage due to numerous flights. They are being upgraded and changed to better protect the payload. Today there are various types of vibration tests and material tests that are done before the launcher and payload can be used.

1.2.4 Payload Fairing Structure

Launch vehicles intended purposes are transporting payloads to orbit. The payload fairing is the most important aspect of the launcher, as it protects the payload during the launch sequence. The fairing has two half-shell bodies that are connected together by the separation system, and they are joined to the upper stage of the launch vehicle [14]. Figure 1.3 below shows the components of a payload fairing and the connection between the second stage and upper stage.

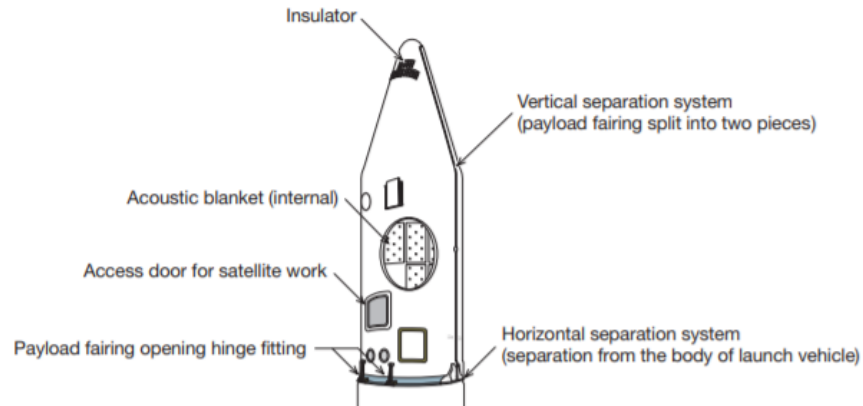


Figure 1.3: Payload fairing system components [14]

Most payload fairings have an access door that is used for securing the payload and any maintenance. Furthermore, there are insulators to prevent any internal heat and an acoustic blanket that reduces any sound vibrations [14]. Payload fairings use a composite material due to their lightweight nature. Another benefit is high strength which increases the rocket's performance [15]. The strength of the material is important to protect the payload. The combination of the lightweight and high strength composite allows for the rocket to travel faster while carrying a heavier payload. New advancements in payload design have resulted in carbon-fiber shells being cured in an industrial oven instead of an autoclave [16]. The new design is stronger, lighter, and has fewer parts. Fairing design is consistently changing to better protect the payload.

1.2.5 Launcher Requirements

Launch vehicles experience a range of stresses and vibrations at various stages of the flight sequence. Generally, a launcher will have a liftoff, transonic flight, and three stages of separation that influence different stresses. Bending and axial modes are experienced during the entire flight sequence. Bending mode is defined as the cross section of a structure that undergoes translation and rotation [17]. The bending mode is affected by the thrust of the engine because the bottom of the rocket is in compression during liftoff and the top of the rocket is in tension. Wind gusts

during flight affect the trajectory of the rocket and create rotational motion which impacts the amount of bending the payload and rocket experience. Axial mode is structural oscillation between two surfaces (horizontal and vertical) [18]. Four components influence the axial mode: thrust, drag, mass and fuselage pressure. Thrust and drag create the most oscillation between the structure of the rocket. The mass of the launcher is defined as the weight of the entire system but the mass in the upper stages create axial modes. As the launcher transitions between stages the mass and center of gravity changes. The upper stages have to counteract the transition to balance the payload. The fuselage pressure changes as the rocket ascends into higher elevation, and the difference between the outside and inside pressure affects the axial mode. Launch vehicles have a range between 5 and 100 Hz for bending and axial modes. Figure 1.4 below shows the main components of a launch vehicle that create axial mode and a general graph of the axial force.

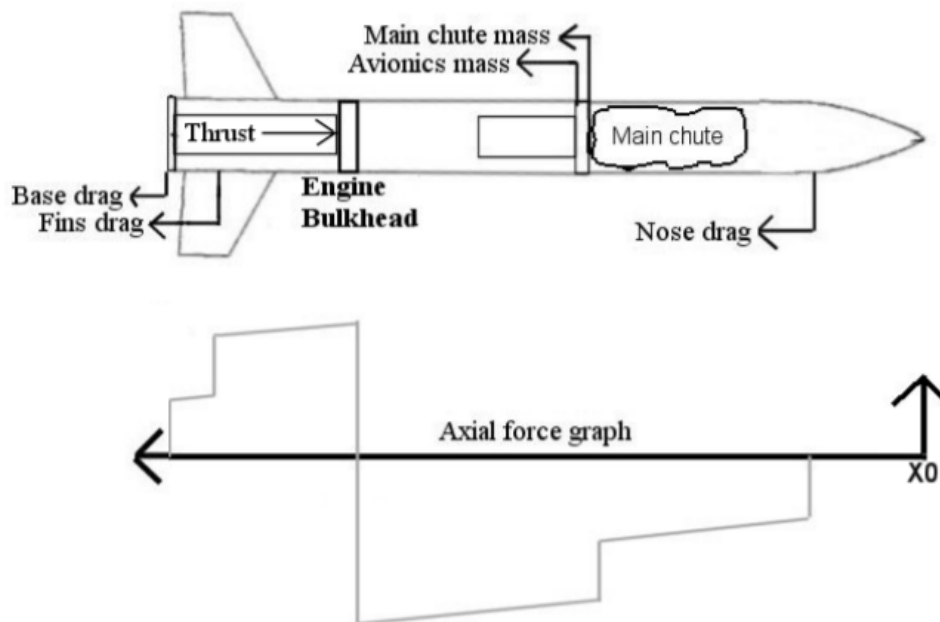


Figure 1.4: General axial force of a rocket [18]

The launch vehicle and payload are subjected to varying thermal environments during the launch sequence. Three subsystems control the thermal environment: cooling for avionics on ground, cooling during launch, and cooling during orbit [19]. At pre-launch a nitrogen duct cools the rocket and disperses the heat through a heat sink. During flight the heat is stored in radiators and upon hitting orbit the heat is expelled through external radiators [19]. All launch vehicle payload fairings are rated below 400 degrees Fahrenheit. Therefore, the requirements for a payload are low compared to what the launch vehicle experiences. Continuing, shock vibration occurs during separation and liftoff. Shock vibration results from quick acceleration and pauses in acceleration. The frequency range of spacecraft shock tests is typically from hundreds to thousands of Hz [20]. The launch vehicle absorbs most of the shock but the payload will still experience shock during separation. Finally, acoustic loads occur during a launch sequence. They are highest during lift off and transonic flight. The load is measured in decibels and creates large vibrations. However,

a payload is usually unaffected by acoustic loads during flight because there is little interaction between acoustic vibration and the payload [20]. Overall, launch vehicles have specific requirements the payload must meet to safely launch into orbit.

1.3 Project Objective

The goal of this project is to understand launcher requirements, general vibration theory, and a finite element analysis on a satellite. The satellite will be modeled to simulate structural vibration and thermal environments during a launch sequence. The results will be compared to modern day launchers vibrational requirements. The results will yield the appropriate launcher to safely deliver the satellite payload into orbit. The thermal, vibrational, and acoustic properties will verify the launcher chosen is correct.

1.4 Methodology

Structural analyses of the spacecraft are performed to verify maximum stresses (thermal and structural such as bending and torsion) and vibrations. These analyses are usually performed using finite element methods, and they determine the feasibility and integrity of the preliminary design of the structure and selection of materials. In this project, finite element analyses will be performed on a mock satellite structure to verify launcher vibrations requirements. Initially, the requirements of different existing launchers are reviewed and compared. Each launcher has different thermal and vibrational requirements that must be met to allow the payload to be transported. Then, a review of vibration theory is conducted to determine general vibrational equations that predict the behavior of single degree of freedom systems, shock vibrations, and acoustic vibrations.

After these initial reviews, a satellite will be modeled in a commercially available finite element software ANSYS. The satellite will be a mock satellite with predetermined dimensions. The pre-analysis of the satellite will verify general structural vibration equations. This preliminary sizing will include material selection for the payload. The analysis in ANSYS will simulate the thermal, and vibrational properties experienced during the launch of a rocket. The results will be compared to modern day launchers requirements, to determine the appropriate launcher.

2.Launcher Structural Requirements

2.1 United States Launch Vehicles

This chapter discusses an in-depth analysis of different countries launch vehicle requirements. Launch vehicles share similar requirements but each country is unique in the way they optimize their requirements for payloads. The United States has the largest barrage of launcher vehicles in the world. Their fleet consists of the Falcon 9, Atlas V, Delta IV, and the Falcon Heavy. The Falcon 9 has become the central focus with advanced technology in launchers because it is the first reusable launcher. The lower stage can be controlled to land itself safely on a pad and be reused. This is one of the many advancements that launchers are achieving today. However, each launcher has different vibrational, thermal, and acoustic requirements that must be met to launch a satellite.

2.1.1 Falcon 9

The Falcon 9 is a launch vehicle designed by SpaceX. It has become the face of launchers because of the ability to reuse the launch rocket. Upon separation the rocket booster can be controlled and landed. The Falcon 9 specifies a design load factor with a fundamental bending mode greater than 10Hz, a fundamental axial mode greater than 25Hz, and a mass between 3,000 and 20,000lbs for a payload [21]. Figure 2.1 below shows the shock environment when the fairing separation occurs as well as the payload separation. The graph has a linear relationship between the acceleration in G-force and the frequency experienced in hertz.

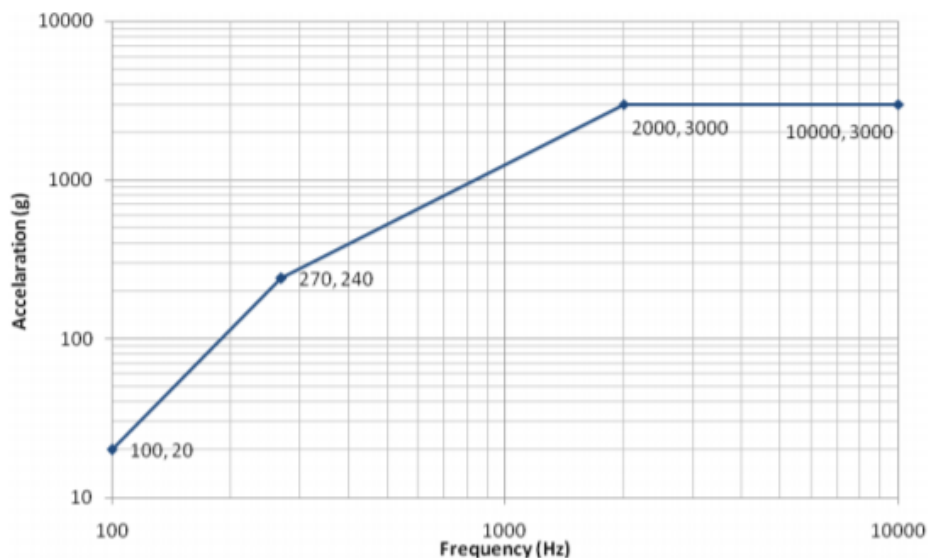


Figure 2.1: Frequency of payload as acceleration increases [21]

The payload only experiences shock during fairing separation and payload separation. During lift-off and 2nd stage separation the launcher itself takes the shock and the payload is unaffected. Continuing, the payload will be subjected to an acoustic environment that is at its peak during lift-off and transonic flight [21]. The Falcon 9 uses a composite structure inside the fairing which significantly decreases the max temperature of the payload to 200 degrees fahrenheit. This launch vehicle is the most important and relevant launcher in the world based on its continuous advancements and technology.

2.1.2 Atlas V

Similarly, the Atlas V launcher requirements are comparable to the Falcon 9. The Atlas V is operated by United Launch Alliance and has been in use since 2002. The design load must meet a payload weight between 2,720 to 20,062 lb with a minimum lateral bending of 8Hz and an axial bending of 15Hz [22]. The Atlas V launcher has five different adapters that are used based on their respective shock requirements. Crew payload has a smaller shock requirement compared to larger payloads such as satellites. The shock levels for each payload adapter are shown in figure 2.2 below. The adapters are designed to optimize the payload requirements, such as crew or satellites.

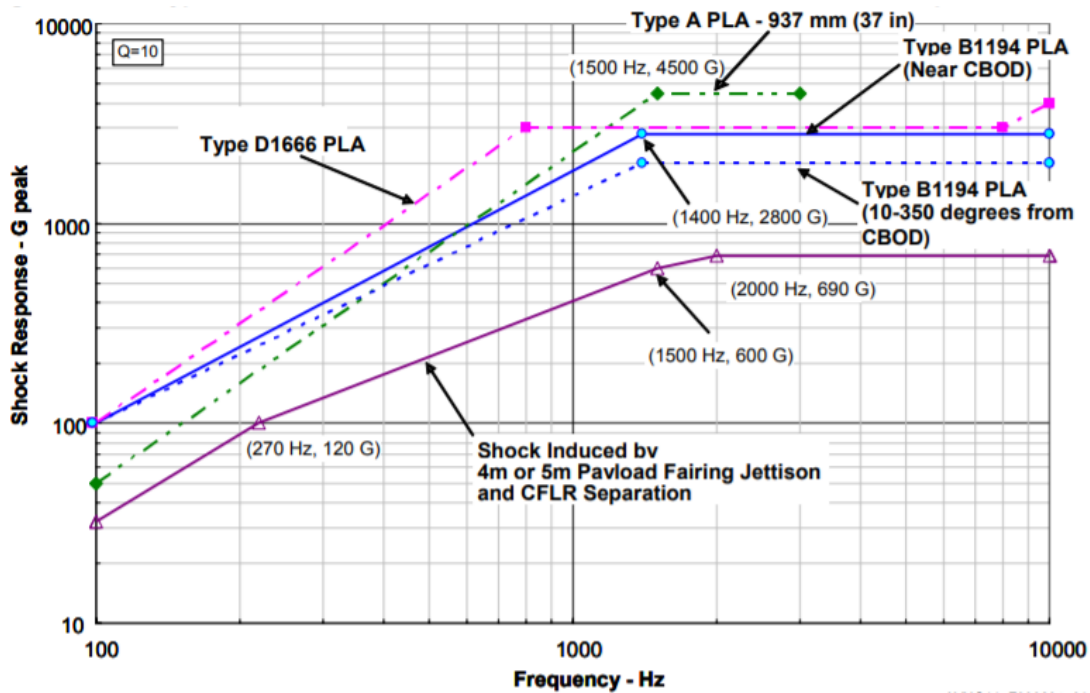


Figure 2.2: Acceleration g-force for each adapter with frequency measured [22]

In addition, the payload experiences the highest acoustic vibration during takeoff and transonic flight. The acoustics are measured on a one third octave band scale for the Atlas V. All payload fairing adapters are equipped with two heat blankets that limit the heat to below 200 degrees fahrenheit [22]. The Atlas V launcher is a unique launch vehicle that has been in use for almost a

decade. The payload attachments allow a greater range of payloads to be delivered into low Earth orbit.

2.1.3 Delta IV

The final launcher the United States uses is the Delta IV. The Delta IV is operated by the United Launch Alliance and has two launch vehicle rockets: the Delta IV M+ and the Delta IV Heavy. The Delta launch family is the smallest launch vehicle in the United States fleet. The M+ is a smaller vehicle which transports small to medium payloads, while the Heavy is used for the bigger payloads. The M+ carries a payload mass between 2000 and 6878 pounds. While the Delta Heavy carries payload up to 10000 pounds [23]. The minimum lateral bending mode for the M+ is 8 Hz and the minimum axial bending mode is 27 Hz [23]. The minimum lateral bending mode for the Heavy is 8 Hz and the minimum axial bending mode is 30 Hz [23]. The shock environment experienced follows the same linear trend of the other U.S. launch vehicles. Similarly with the other two launches, the Delta IV max acoustic environment is during takeoff and transonic flight. Continuing, the payload experiences a higher temperature relative to the other launchers of 220 degrees Fahrenheit [23]. The three launchers in the United States with available data show similar requirements but have different functionalities and performance criterias.

2.2 Russia Launch Vehicle

In contrast to the United States, Russia has one launch vehicle that has been re-designed and engineered over the last three decades. It was originally designed in the 1980's to replace the Soviet Union's Proton family [24]. It consisted of a two stage rocket booster until the early 2000's. The latest version of the Zenit launcher is the 3SL. The 3SL is a three stage rocket booster that has three different payload fairing attachments. The fairing attachments are used for different payload types to limit the structural vibration imposed on the payload.

2.2.1 Zenit

The Zenit 3SL is the latest variation in the Zenit family. It is a medium lift vehicle which is capable of carrying a payload between 3500 and 26500 pounds [24]. The lateral and axial vibrations must be between 5 and 100 Hz [24]. The Zenit launcher, similar to the Delta, has different adapters for shock vibration control based on the payload. Figure 2.3 below shows the three adapters and the g-force they experience measured against the frequency response. The three interfaces are designed for separate tension to control the payload. The band tension is determined before launch based on the weight of the payload and the distance required for the mission.

Frequency (Hz)	Shock Response Spectra (g)							
	937 Interface			1194 Interface				1666 Interface
	Band Tension (kN)			Band Tension (kN)				Band Tension
	12.5	20	30	10	20	30	40	30 kN
100				50	50	50	60	150
200	60	60	60	130	130	140	170	400
800	550	600	650	800	900	1150	1450	3,000
1300	1150	1300	1550	1500	1800	2400	3000	3,000
2000	2300	2700	3300	1850	2250	3000	3750	3,000
3000	2600	3050	3750	2300	2750	3600	4600	3,000
3500	2700	3150	3900	2500	3000	4000	5000	3,100
6000	3200	3700	4600	2500	3000	4000	5000	3,500
8000	3500	4000	5000	2500	3000	4000	5000	3,500
9000	3500	4000	5000	2500	3000	4000	5000	3,500
10000	3500	4000	5000	2500	3000	4000	5000	3,800

Figure 2.3: Frequency response of different adapters and the g-force experienced [24]

The maximum acoustic vibration occurs during takeoff and transonic flight. Each payload fairing has a thermal blanket that limits the heat exposure to 210 degrees Fahrenheit [24]. The Zenit launcher has been developed and redesigned for the last three decades and the different payload fairings allowed the launcher to have a large variety of payload.

2.3 Europe Launch Vehicles

Europe has two launch vehicles, the Vega and Ariane 5. Both launchers are produced by the same company ArianeSpace, so the requirements are similar for both launchers. However, the Vega is much smaller than the Ariane 5 and is used for smaller payloads. The Vega launcher is co-operated by the Italian Space Agency and the European Space Agency. It began development in 1998, and the first launch was in 2012 [25]. The Ariane 5 is Europe's heavy launch vehicle. It has had 82 consecutive launches since 2003, and has eight launches left until the Ariane 6 replaces it [26]. Europe utilizes two launchers to optimize the payload range without having to manufacture separate payload fairings like the Zenit launcher does.

2.3.1 Vega

The Vega is a small launch vehicle that can carry a payload weight between 700 and 2500 pounds [25]. It has a design load with a minimum lateral bending of 15 Hz and a minimum axial bending mode of 20 Hz [25]. The Vega transports small satellites and crew into low Earth orbit, but its functionalities are limited due to the size of the launcher. The shock response is shown in figure 2.4 below. The graph follows the same linear pattern as the previous launchers. As the shock level increases the frequency increases, until it reaches the max level for the payload.

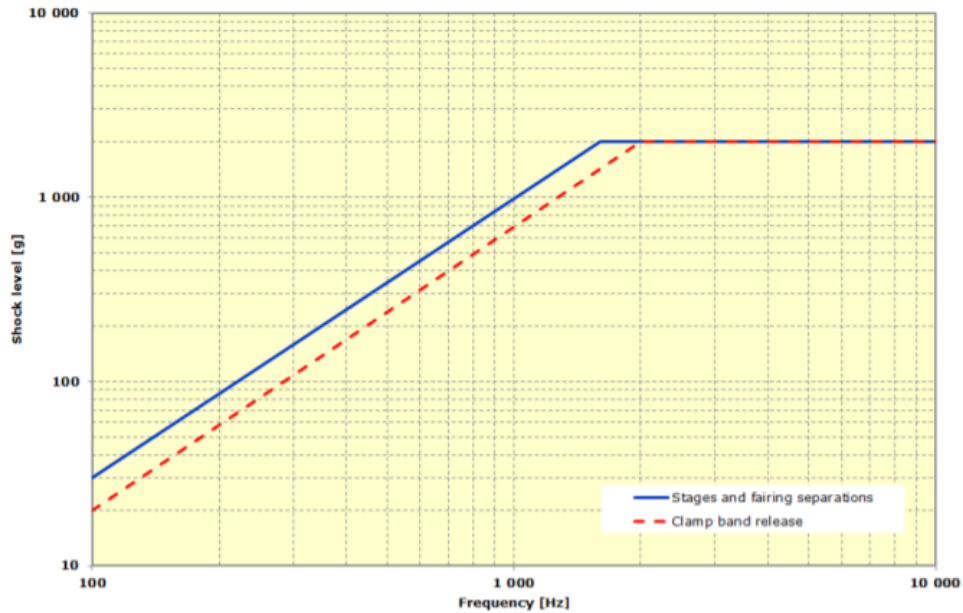


Figure 2.4: Frequency of payload as shock g-force increases [25]

The acoustic levels are at the max during takeoff and transonic flight and negligible elsewhere. The payload is subject to a max temperature of 200 degrees Fahrenheit [25]. Based on the size of the Vega, the requirements are much lower for the payload compared to other launch vehicles around the world.

2.3.2 Ariane 5

The Ariane 5 is Europe's biggest launch vehicle and used more frequently. It will complete over 90 launches before it is retired for the Ariane 6 in the coming years. The Ariane 5 is capable of carrying a payload up to 25000 pounds [26]. It has a design load with a minimum lateral bending of 2 Hz and a minimum axial bending mode of 15 Hz [26]. Figure 2.5 below shows the shock response of the payload relative to acceleration. The relationship of the shock environment in the Ariane 5 is different from other launch vehicles. The linear relationship between frequency and the shock level occurs until the max shock is reached. However, the shock vibration begins to decrease based on the payload fairing design.

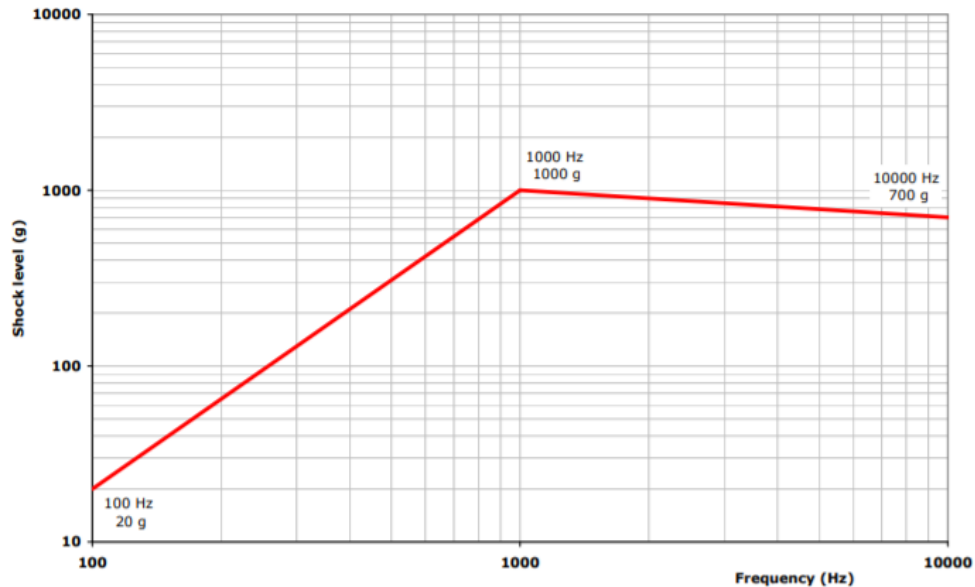


Figure 2.5: Shock response relative to acceleration [26]

Similarly to all acoustic vibrations with launch vehicles, the max acoustic vibration occurs during takeoff and transonic flight. The payload fairing limits the max temperature to 210 degrees Fahrenheit. The Ariane 5 is Europe's largest and most successful launch vehicle. The design has proved to limit shock vibration for payloads and create a safer and powerful launch vehicle.

2.4 China Launch Vehicle

China is the last country with a launch vehicle family that is readily available and used frequently. The launchers used are the Long March. There are over 20 different launchers in the family that have been used and developed. The first initial launcher was developed in 1970 [27]. Today there are 10 that are actively being used to deliver payload. The biggest launcher in the group is the Long March 3B. However data is only available for the 3A.

2.4.1 Long March

The Long March family is an extensive group of vehicles that have been redesigned to perform at the highest level. The launchers can carry a payload up to 26000 pounds and the fairing won't exceed 186 degrees Fahrenheit [27]. However, the Long March 3A can carry a payload up to 16000 pounds [27]. The Long March has multiple adapters that can be utilized depending on the mission and the payload size. The design load of all adapters is a minimum lateral bending of 5Hz and a minimum axial bending of 8 Hz [27]. Figure 2.6 shows the shock vibration graph. The curve follows the same linear trend that all launchers follow. The shock vibration increases until it maxes and stays on a horizontal trend.



Figure 2.6: Frequency of shock vibration against g-force acceleration [27]

The max acoustic vibration occurs during takeoff and transonic flight. The Long March family has a vast supply of launch vehicles that are similar to most other countries launchers. Overall, the requirements for all launchers are different in some way, and the countries have optimized their desired method of transporting payload to Low Earth Orbit.

3. Vibration Equations

3.1 SDOF with Moving Base

Machines and machine parts can be modeled using the base excitation theory, where the harmonically elastic mounting can be viewed as a spring. Within a spacecraft the payload is excited through the acceleration of the launch vehicle. Summing the forces acting on the payload mass results in the internal forces being equal to the gravitational forces and the static deflection. Figure 3.1 below is the setup for the single degree of freedom with a moving base example. The mass is modeled with a spring and damper that moves vertically over a change in time. The displacement of the position is dependent on the spring constant, and the change in velocity is dependent on the velocity of the damper. The payload fairing can be modeled using a single degree of freedom because it is elastically bound to the launch vehicle. Therefore, the payload will experience harmonic motion as it accelerates.

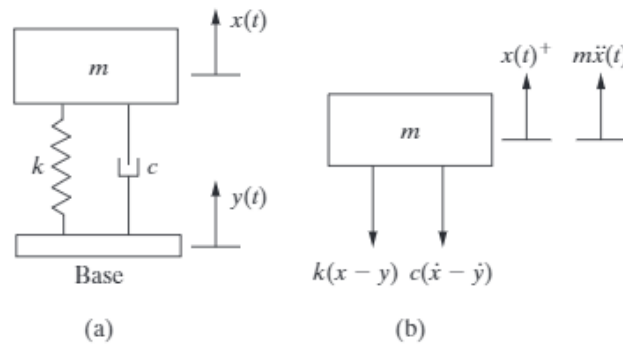


Figure 3.1: Mass with moving base example [28]

Equation 1 below shows the single degree of freedom equation that a payload experiences. It is a second order differential equation.

$$m \ddot{x} + c(\dot{x} - \dot{y}) + k(x - y) = 0 \quad (1)$$

The spring deflects a distance $(x - y)$ and the damper experiences a velocity of $(\dot{x} - \dot{y})$. The $m\ddot{x}$ variable is the inertial force the payload experiences. A spacecraft can be assumed to move harmonically throughout the launch sequence. Equation 2 below denotes a harmonically moving base. Y is the amplitude of the base motion and w_b is the frequency of base oscillation.

$$y(t) = Y \sin w_b(t) \quad (2)$$

Equation 1 and 2 can be combined to form the spring-damper system with two harmonic inputs [28]. Equation 3 below is the final equation that can be solved using the linearity of the equation of motion to obtain the particular solution of the payload motion.

$$m\ddot{x} + c\dot{x} + kx = cYw_b \cos w_b t + kY \sin w_b t \quad (3)$$

The spring damper system has two inputs that create two particular solutions. One solution is based on the cosine of the function, while the other solution is based on the sine function. Equation 4 and 5 below show the particular solutions. The solution to equation 3 is the sum of equation 4 and 5.

$$x_p(1) = \frac{2\zeta w_n w_b Y}{\sqrt{(w_n^2 - w_b^2)^2 + (2\zeta w_n w_b)^2}} \cos(w_b t - \theta_1) \quad (4)$$

$$x_p(2) = \frac{w_n^2 Y}{\sqrt{(w_n^2 - w_b^2)^2 + (2\zeta w_n w_b)^2}} \sin(w_b t - \theta_1) \quad (5)$$

Both equations use the same variables, where Y is the amplitude of the base motion. The difference between the two is taking the cosine and sine of the phase angle theta. The phase angle is independent of the base excitation, but the damping ratio, natural frequency, and the frequency of the base oscillation [28]. Equation 6 below shows the general solution or magnitude of the particular solutions.

$$\frac{|x_p(t)|}{Y} = \left[\frac{1 + (2\zeta w_n w_b)^2}{(1 - (w_n w_b)^2)^2 + (2\zeta w_n w_b)^2} \right]^{1/2} \quad (6)$$

The general solution computes the displacement ratio against the frequency ratio for a moving base. The damping ratio is the variable that is adjusted and the solution can be plotted with various damping responses.

3.2 Sinusoidal Vibrational Load with Moving Base

Spacecraft experience a sinusoidal vibration load due to the acceleration. Sinusoidal vibration is defined as the vibration that the structure excites by the forcing with a pure acceleration and one frequency [29]. Sinusoidal vibration is not common, and is a special form of vibration but always provides an understanding of complex vibrations when it's broken down into one tone vibration [29]. Payloads are tested before they are placed inside a fairing and must meet the launch vehicles specific requirements. The tests are complex and are based on the shock and random vibrations experienced during launch. Figure 3.2 below shows a typical sinusoidal vibration

profile. The displacement of the structure is measured as the frequency of the vibration is increased.

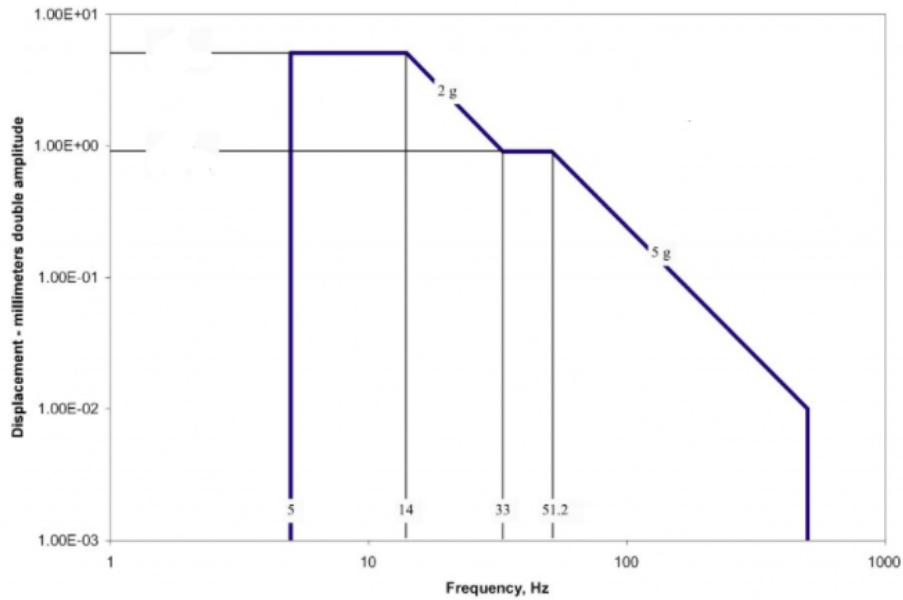


Figure 3.2: Basic sinusoidal profile for a spacecraft structure [29]

Example 3.2.1: A general example of the Falcon 9 specifies a payload of 5000 kg, a natural frequency of 30 Hz, a damping ratio of 0.1, and a base amplitude of 0.03m. The frequency of base oscillation is varied from 5-200 Hz. The numbers were selected based on the given ranges for all the launch vehicles in chapter 2. The numbers fall into the selected range of given requirements.

$$\text{Stiffness: } k = m * \omega_n^2 = 1.77 * 10^8 \text{ N/m}$$

$$\text{Particular solution 1, } \omega_b = 31.42 \text{ rad/s: } x_p(1) = .000925 \text{ mm}$$

$$\text{Particular solution 2, } \omega_b = 31.42 \text{ rad/s: } x_p(2) = .0287 \text{ mm}$$

$$x_p(1) + x_p(2) = .02971 \text{ mm (single amplitude)}$$

$$\text{Double amplitude} = 0.05942 \text{ mm}$$

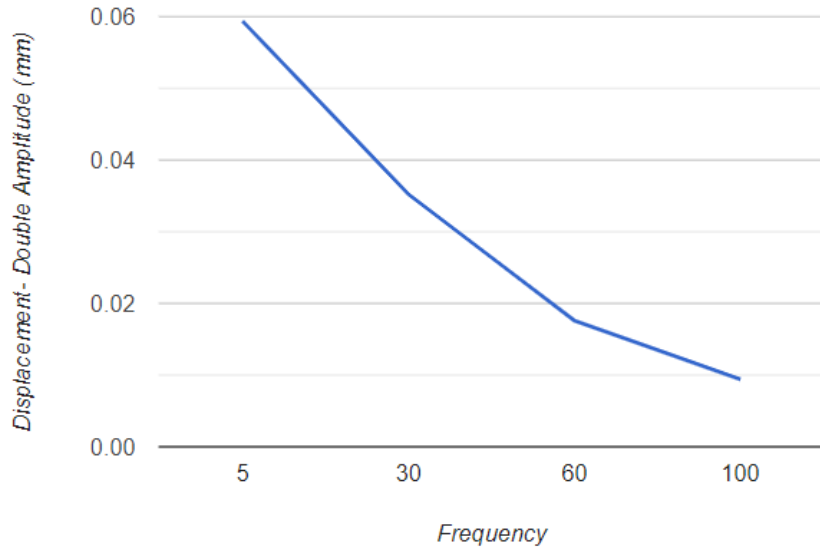


Figure 3.3: Sinusoidal profile for example 3.2.1

The amplitude is defined over a range of frequencies during the test, it can be constant or variable [29]. During a sine vibration test, the vibration waveforms are swept through a range of frequencies that pass through the structure. The displacement increases as the frequency decreases for a given acceleration [29]. The purpose of this test is to find the resonances in the structure. It verifies the structural integrity of the payload and ensures that it can safely handle the acceleration of the launch.

3.3 Random Vibrational Loads

Random vibrational loads are measured based on a force input over time. Disturbances in spacecraft are characterized as random if the value of $F(t)$ for a given value of time is known only statistically [28]. Random vibrations have no pattern and are difficult to measure. However, the disturbances can be analyzed measuring how fast the displacement, $x(t)$, changes over time. Equation 7 below is the autocorrelation function, R_{xx} . It is the first step in measuring random vibrations, because it measures how fast a variable(structure) changes.

$$R_{xx}(\tau) = \lim_{T \rightarrow \infty} \frac{1}{T} \int_0^T x(t)x(t + \tau)dt \quad (7)$$

The equation is a measure of how fast $x(t)$ changes over time. The term, $x(t)x(t + \tau)$, is taking two sample measurements at a time, t , and evaluating the difference at a time difference, τ [28]. Taking the Fourier transform of the autocorrelation function above, defines the power spectral density (PSD) [28]. Equation 8 below shows the power spectral density equation.

$$S_{xx}(w) = \frac{1}{2\pi} \int_{-\infty}^{\infty} R_{xx}(w) e^{-jw\tau} d\tau \quad (8)$$

From equation 7 and 8, a system transfer function is obtained for a single degree of freedom and shown in equation 9 below. This is the set equation for solving the random vibrations of a spacecraft. Equation 9 is the transfer function of a single degree of freedom problem.

$$H(s) = \frac{1}{ms^2 + cs + k} \quad (9)$$

Following the transfer function, the final equation to solve random vibrations is listed in equation 10 below.

$$S_{xx}(w) = |H(w)|^2 S_{ff}(w) \quad (10)$$

The variable $S_{ff}(w)$ denotes the power spectral density of the forcing function. $H(w)$ is the solution of the transfer function squared, which represents the magnitude of the complex frequency response [28]. Overall, a few equations can help numerically solve random vibrations. However, a finite element analysis of the payload must be performed to properly analyze random vibrations.

Example 3.3.1: Calculate the $S_{xx}(w)$ for a single degree of freedom with a general force of $F(t)$.

$$\text{Equation of motion: } m\ddot{x} + c\dot{x} + kx = F(t)$$

$$\text{Frequency Response function: } H(w) = \frac{1}{k - mw^2 + cwj}$$

$$S_{xx}(w) = |H(w)|^2 S_{ff}(w)$$

$$\text{Complex Frequency Response: } |H(w)|^2 = \left(\frac{1}{k - mw^2 + cwj} \right)^2 = \frac{1}{(k - mw^2)^2 + c^2 w^2}$$

$$S_{xx}(w) = \frac{S_{ff}(w)}{(k - mw^2)^2 + c^2 w^2}$$

3.4 Shock Vibration Loads

A sudden result of force or any other form of a disturbance resulting in a transient response is referred to as a shock vibration [28]. The shock spectrum creates a maximum value of the system's time response versus the natural frequency, as seen in chapter 2. Equation 11 below shows the response of a system to any input of force.

$$x(t) = \int_0^t F(\tau)h(t - \tau)d\tau \quad (11)$$

The force is measured against a time difference tau. The variable $h(t - \tau)$ is the impulse response for a shock vibration [28]. Equation 12 below, is used to obtain the shock response graph. It takes the sine of the natural frequency times the time difference. The equation allows different force inputs to accurately obtain the graph for the given force.

$$x(t)_{max} = \frac{1}{mw_n} \left| \int_0^t F(\tau) \sin[w_n(t - \tau)] d\tau \right|_{max} \quad (12)$$

Example 3.4.1: The falcon 9 has a payload mass of 5000 kg and a range of frequencies from 100-10000 Hz. The force due to acceleration is defined as: $F_1(t) = \frac{t}{t_1}F_0$. $F_0=49,050$ N.

Solving Equation 3 for max acceleration: $\ddot{x} = 3000$ g's
 From equation 11 at 100 Hz: Acceleration Force= 100 g's
 From equation 11 at 240 Hz: Acceleration Force= 270 g's

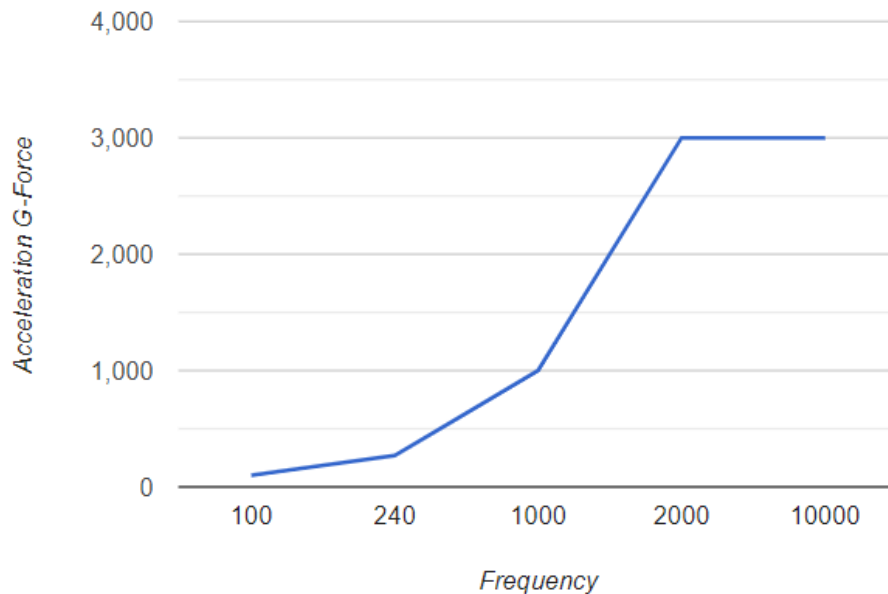


Figure 3.4: Falcon 9 shock response from example 3.4.1

The Falcon 9 follows a linear curve, so obtaining the max acceleration force allows equation 11 to be back solved to obtain the initial force. Equation 12 is used to verify the max force against the max displacement. Refer to figure 2.1 for the plot of the Falcon 9 shock response.

Calculating the shock response involves substituting the range of $F(t)$ into equation 8 and plotting $x(t)_{\max}$ versus the undamped natural frequency [28]. Therefore, the shock response can be easily plotted given the appropriate variables and force range. The solution can be calculated by hand or be done using finite element analysis.

3.5 Finite element analysis

The sections above lay the baseline for numerical analysis of structural vibrations. However, the payload must be modeled in a computer software program to accurately model vibrations during launch. Finite element analysis predicts real world vibrational effects and displays where a structure will experience the greatest force [30]. It shows strengths and weaknesses and allows the product to be changed to safely be used. The first step of using FEA is to create a mesh which breaks down the model into millions of small elements that are refined to make up the dimensions of the shape. The simulation can be run following the mesh of the structure. FEA uses partial differential equations with multiple degrees of freedom to accurately model the vibrational forces. The equations provide graphs and numerical data which are used to analyze the structure.

4. Mesh and Sinusoidal Analysis

4.1 Geometry of Satellite

The model of a monoblock satellite was created in Ansys Spaceclaim. The structure is shown below in figure 4.1. A monoblock satellite was analyzed to limit the complexity of the solution compared to modern day satellites.

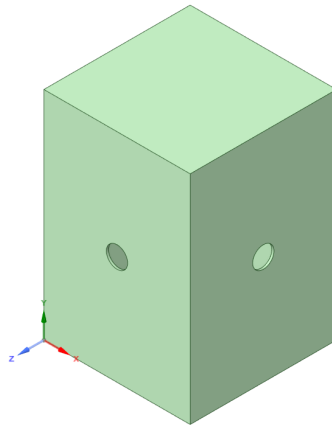


Figure 4.1: Isometric view of monoblock satellite

The structure is a symmetrical rectangular block with four holes on each side face. The holes are used to store or remove payload components within the satellite, as well as thermal dissipation during the launch sequence. The side faces are a rectangle with a length of 1530 mm and a width of 1030 mm. The hole has a diameter of 150 mm and is 515 mm from the top and side of the satellite. The thickness of each face is 15 mm and all four faces are identical. The top and bottom face are identical and are a square. It is a 1030 mm by 1030 mm shape with a thickness of 15 mm. The dimensions of the side faces and the top face are shown in figure 4.2 below.

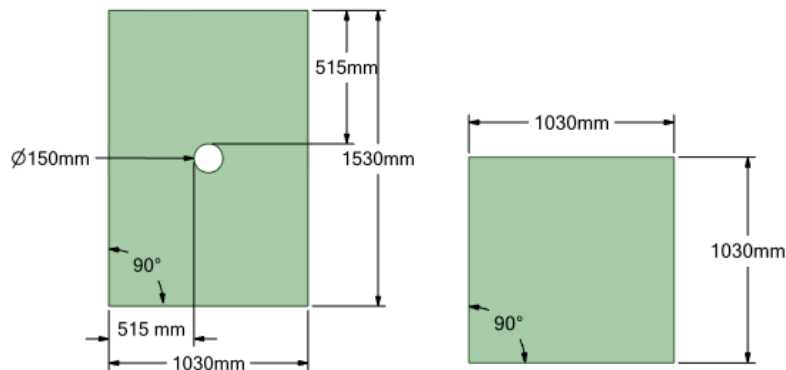


Figure 4.2: Side view (left) and top view (right)

4.2 Modal Analysis and Mesh Verification

A. Modal Analysis

An initial modal analysis of the monoblock satellite was performed in Ansys. The material selected was Aluminum alloy, wrought, 6061, TI and was distributed evenly throughout the structure. The analysis was performed at 22 C. Inside the satellite a spring mass system was created to simulate a payload mass of 5000 kg, based on the average weight limits of all the launch vehicles. The spring value remained constant from the data obtained in section 3.2. Figure 17 below shows the spring-mass system, which is attached to the top face of the monoblock satellite.

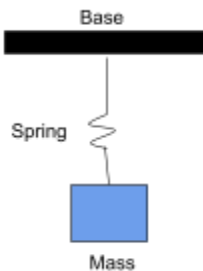


Figure 4.3: Spring-mass system within satellite

During launch, the payload will experience a vibrational response that can be modeled using a spring. The monoblock was simulated with a fixed support at each corner of the structure at the top and bottom face. The satellite will be fixed within the payload fairing. The initial mode shapes (1-7) of the monoblock satellite are shown in figure 4.4 and 4.5 below. Table 4.1 shows the natural frequencies for each mode shape.

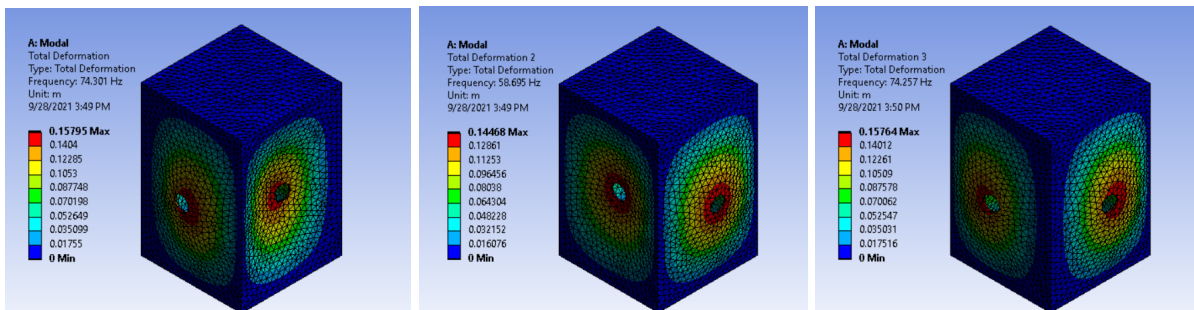


Figure 4.4: Mode shapes 1-3

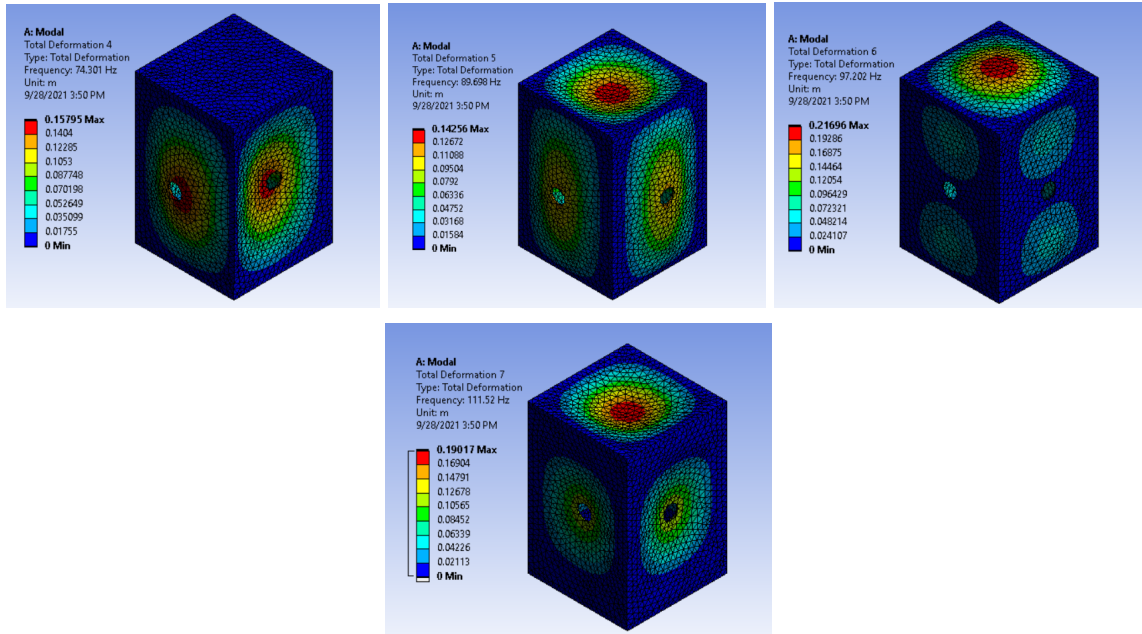


Figure 4.5: Mode shapes 4 (top left)-7(bottom)

Table 4.1: Natural frequency of each mode shape

Mode Shape	Natural Frequency
1	58.695
2	74.247
3	74.301
4	89.698
5	97.202
6	111.520
7	123.624

B. Mesh Verification

Multiple natural frequencies and mode shapes are computed to ensure the mesh is refined enough for the requirements. Ansys generates meshes using tetrahedron elements. Each mesh test case was solved using the same design parameters as the modal analysis. Table 4.2 below shows the 9 test cases of the mesh verification.

Table 4.2: Mesh verification parameters

Test Case	Element Size(m)	Element Type	Linear/ Quadratic	Element Number	Nodes
1	0.1	Tetrahedron	Linear	12,189	5,231
2	0.1	Tetrahedron	Quadratic	3,974	15,231
3	0.05	Tetrahedron	Linear	12,341	5,568
4	0.05	Tetrahedron	Quadratic	4,123	19,752
5	0.025	Tetrahedron	Linear	23, 567	6,141
6	0.025	Tetrahedron	Quadratic	23,368	49,954
7	0.1	Hexahedral	Quadratic	1,420	9,854
8	0.05	Hexahedral	Quadratic	3,126	17,423
9	0.025	Hexahedral	Quadratic	5,845	41,634

Based on the information above, the monoblock satellite reaches grid independence from a quadratic solution at a lower element count compared to the linear solution. Figure 4.6 below shows the mode shapes for the quadratic tetrahedron solution and the hexahedral solution. The modes converged faster to a smaller element size for the tetrahedral solution. There is some error due to the computational power of Ansys but the solution converges to enough to use this mesh type. The quadratic tetrahedron with a 0.05 m element size was chosen for this model. The given mesh is shown in figure 4.7 below.

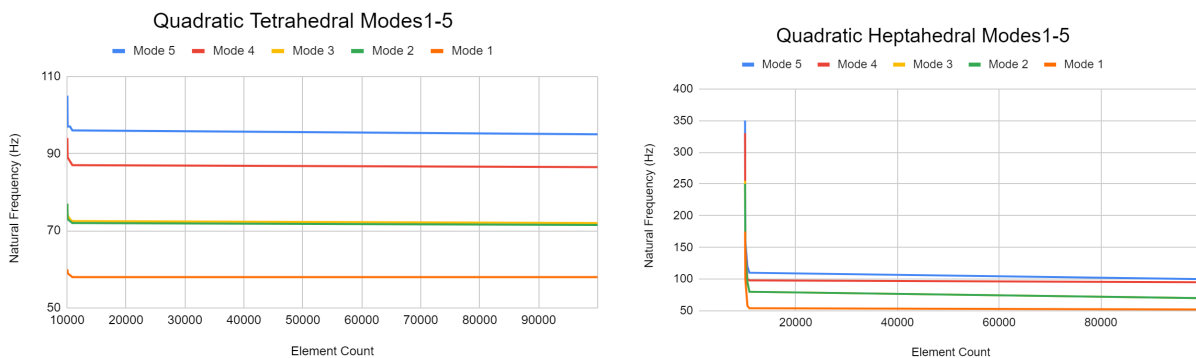


Figure 4.6: Mode convergence for tetra and hexa mesh

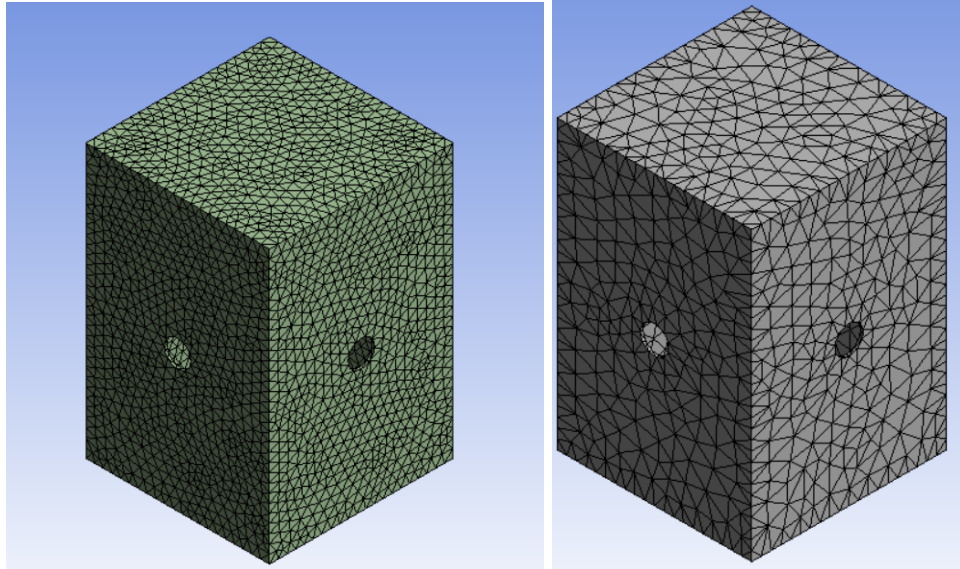


Figure 4.7: Linear(left) and tetra quadratic mesh(right)

4.3 Sinusoidal vibration load

All launcher vehicles specify testing the sinusoidal vibration load before being launched. In the United States the Ground Vibration Laboratory is the primary testing site due to their frequency range of 5-30000 Hz. In Ansys the harmonic response tool is used to simulate the sinusoidal vibration load. Before performing the test the modal analysis is conducted and the data from section 4.2 is pre-loaded into the harmonic response. The max amplitude is the max displacement of the satellite, and is found by sweeping a sinusoidal frequency through the monoblock satellite. Figure 4.8 below shows the response of the spring-mass system within the satellite. The time step was set at one second and the excitation frequency was set at 30hz. The frequency was chosen based on the fundamental axial bending and the given range of test laboratories. The resulting displacement was found to be 0.048mm in the positive y-direction and 0.05mm in the negative y-direction.

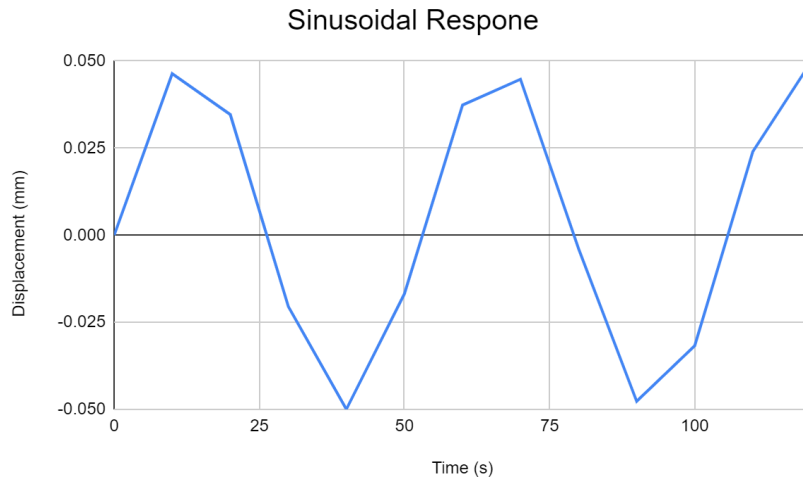


Figure 4.8: Sinusoidal response of monoblock satellite

The data was exported from Ansys to create a sinusoidal graph to show the displacement of the spring-mass system in the monoblock satellite. If the frequency is lowered the data produced does not follow a sine wave pattern and the data shows the satellite will not experience more than 0.01mm of displacement. The frequency of 30hz proved to be the most accurate sinusoidal response. The graph shows that the monoblock satellite will withstand any sine wave structural vibration that the payload experiences. Figure 4.9 below shows the sinusoidal profile of the monoblock satellite. The displacement of the payload is measured over a range of frequencies. As the frequency is increased the displacement linearly decreases. The data is consistent with the computed values in section 3.2. Figure 4.10 shows the double amplitude displacement of the same sinusoidal profile.

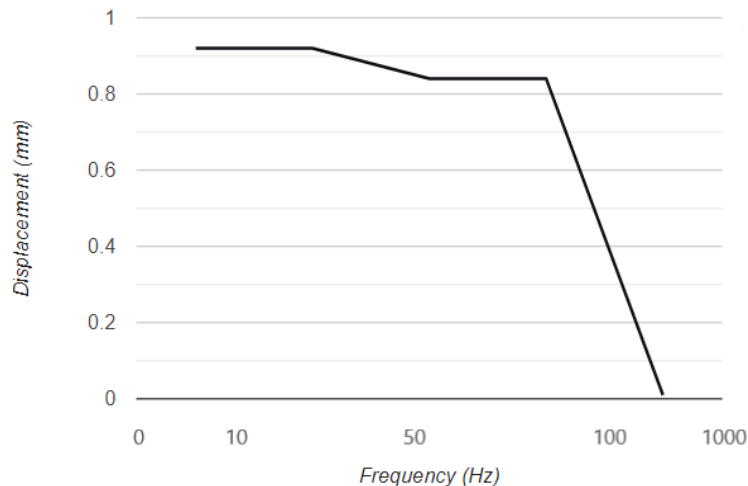


Figure 4.9: Sinusoidal profile of monoblock satellite

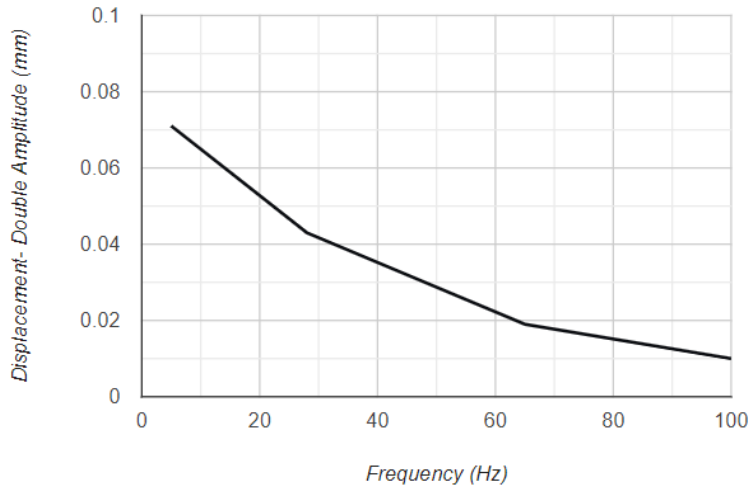


Figure 4.10: Double amplitude of sinusoidal profile

All launcher vehicles listed in Chapter 2 don't provide all the data necessary to compare the sinusoidal response. The displacement and double amplitude displacement can be found exporting the data of the sinusoidal response, and compared with the computed graphs and data in section 3.2. However, the shock response in Chapter 5 has a direct correlation to the sinusoidal function.

5. Shock and Random Vibration Analysis

5.1 Shock Vibration Analysis

The shock loads in the payload structure are generated in short durations during separation of stages and the separation of the payload from the rocket boosters. The duration of the shock load is very short with respect to the fundamental natural frequencies of the mechanical system [4]. Launch vehicles have the heaviest loads upon launch resulting in higher shock loads. After the first stage separation the weight of the launcher is reduced dramatically which creates lower shock loads within the payload. The shock loads are measured in a shock response spectrum graph, refer to section 2.1.1 figure 5. Ansys measures the acceleration based on initial values, damping ratio, and the material selected. The initial values were set at zero to simulate the spacecraft not moving. A damping ratio of 0.05 was used based on the requirements preset from all launch vehicles. The load was set at 5000kg and the point of measurement was selected on the mass-spring system within the satellite. The simulation took a few minutes with a time step of 0.1 seconds. Figure 5.1 and table 5.1 below shows the shock response data of the monoblock satellite generated from Ansys.

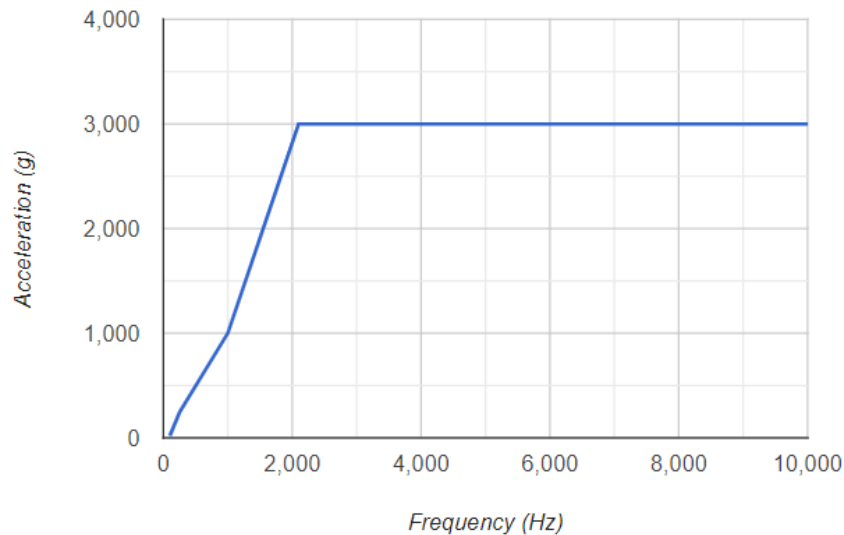


Figure 5.1: Shock response from acceleration of monoblock satellite

Table 5.1: Shock response data from acceleration profile

Frequency (Hz)	Acceleration (g)
100	20
255	250
620	860
1000	1000
2100	3000
10000	3000

The data reveals that the shock load falls within the limits of the Falcon 9 launcher. The max frequency of 10,000 Hz is reached at 3,000 G-force which is consistent with the launcher requirements. The graph follows the anticipated curve based on the different stages of separation. The linear curve increases much faster in the beginning due to the liftoff and burn time of the initial rocket boosters. Upon separation of the boosters the curve begins to level out until it reaches its max value of acceleration. Figure 5.2 below shows the SRS acceleration curve which is the largest absolute response of the system. The shock spectrum takes the acceleration of the system and measures it against the frequency over the time domain. The data obtained was extracted from Ansys and plotted to show the pattern of the SRS. The data obtained shows similarities to other SRS graphs but Ansys is limited in providing an accurate curve.

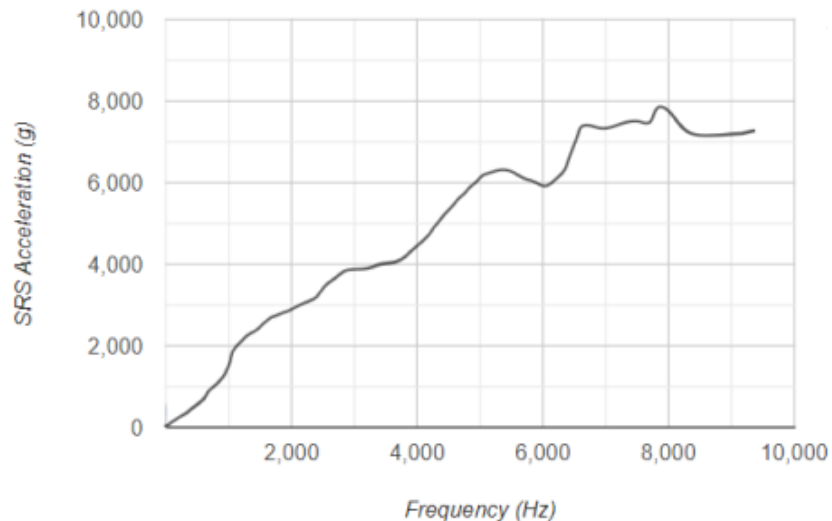


Figure 5.2: SRS acceleration curve

5.2 Random Vibration Analysis

Acoustic loads and boundary layer turbulence are transferred into mechanical loads in a launch vehicle [4]. Random vibrations are often associated with instruments and equipment within the payload fairing, and for this case the monoblock satellite can be analyzed. The random vibration of a satellite is measured using the power spectral density (PSD). Power spectral density is the mean square value of a signal over a spectrum of frequencies. For launch vehicles the units are a measurement of acceleration over frequency (g^2/Hz). Figure 5.3 below shows an example of the Falcon 9/Heavy's minimum random vibration requirements. The graph is the only available random vibration data for the selected launch vehicles. The blackline shows the maximum predicted random vibration of the payload compared to the minimum random vibration spectrum.

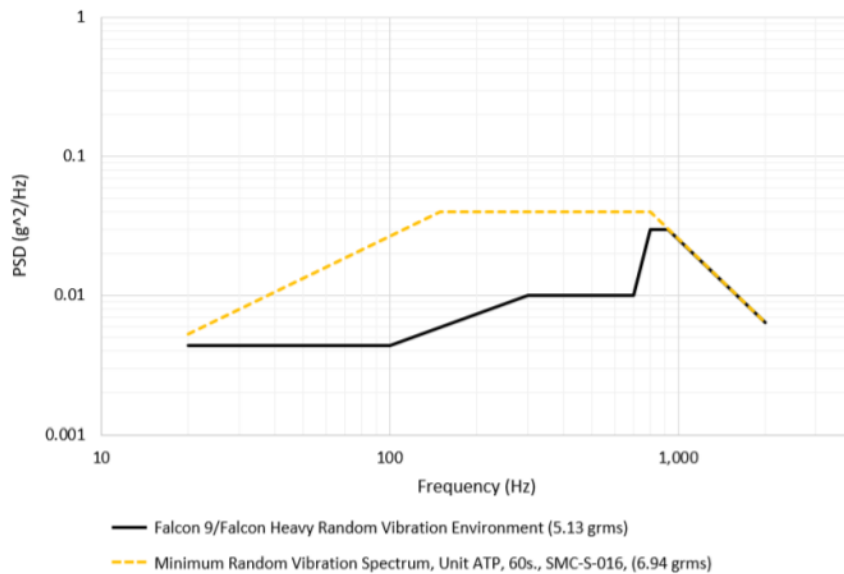


Figure 5.3: Falcon 9/Heavy random vibration example [31]

The random vibration analysis is broken down into three sections. The low frequency section (0-100Hz) is driven by excitation and general motion of the launch vehicle. The mid frequency section (100-600Hz) is excitation from acoustics and the high frequency section (600-2000Hz) is primarily driven by the structure borne vibration [31]. Two simulations were performed to show the differences in the random vibrations on the payload and the top of the monoblock satellite. Figure 5.4 shows the graph of the random vibration conducted at the top face of the satellite. The simulations were conducted using a time step of 0.1 seconds and used the data from the sinusoidal simulation. Ansys allows the simulations to be connected to influence the factors of the random vibration. The two simulations were different in the selection of the applied random vibration location. The data was held constant throughout both however, the satellite will experience a different random vibration load compared to the actual payload within the satellite. The purpose of this was to show that the initial PSD of the graph does not change and shows similarities between the two.

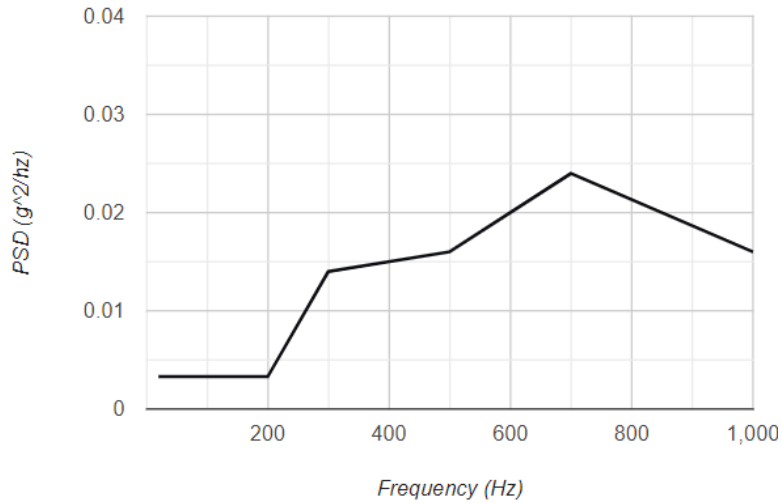


Figure 5.4: Random vibration at the top face of the satellite

The top of the payload fairing follows a similar pattern to the predicted random vibration requirements. At low frequencies the PSD is constant but when it reaches the acoustic zone the PSD of the fairing increases based on the launch and exposure of the nose. The pattern is not identical due to the acoustics not accurately being measured through Ansys. More importantly, the random vibration of the mass spring system must be analyzed to see the difference in the random vibration of the top of the monoblock satellite and the mass spring system. Figure 5.5 and table 5.2 show the data of the random vibration from the mass spring system within the monoblock satellite.

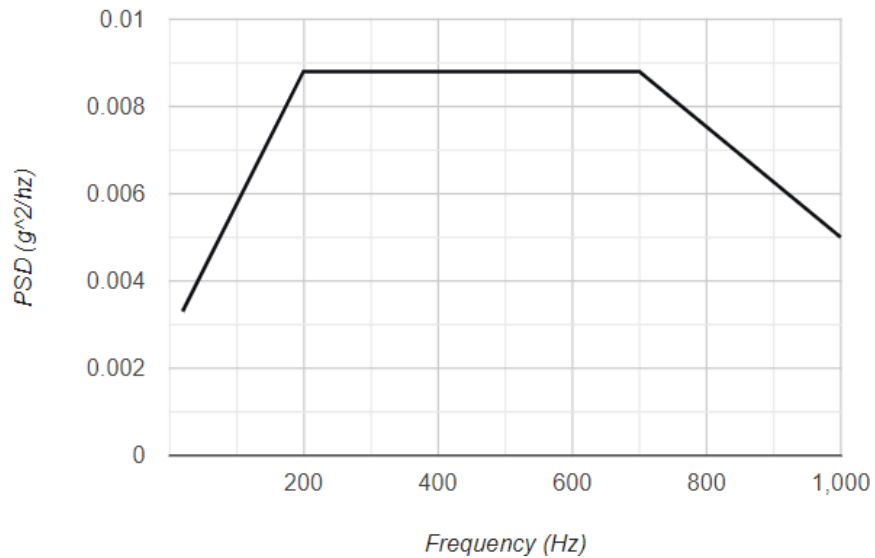


Figure 5.5: Random vibration of mass-spring system

Table 5.2: Data of random vibration

Frequency (Hz)	PSD (g^2/Hz)
20	0.0033
200	0.0088
300	0.0088
500	0.0088
700	0.0088
1000	0.005

The random vibration of the mass-spring system shows a different path because of the oscillations and movement of the system at low frequencies. It experiences random vibrations until it reaches the acoustic stage, where Ansys models a constant frequency for the simulations. However, to accurately measure the random vibration of the monoblock satellite an acoustic test would need to be performed to fully account for all random vibrations. Ansys does not contain the tools needed to model acoustic vibrations and the test would be performed in a lab before determining the final analysis.

6. Conclusion

The monoblock satellite modeled in this project was a baseline for the complexity of structural vibration analysis in satellite systems. The observed data revealed that the Falcon 9 launch vehicle would be suitable for launching the monoblock satellite safely into space. The modal analysis showed grid independence was reached with a quadratic solution, and this mesh was used for all structural vibration simulations. Following the modal analysis, the sinusoidal load was computed. Three graphs were made to show the displacement and double displacement of the payload. The results yielded similar trends to the equations in section 3.2. However, Ansys is limited in the accuracy of the sinusoidal load. The shock and random vibration simulations produced adequate data which was in line with the general launcher vehicle requirements. The simulations revealed that the monoblock satellite was capable of withstanding a launch given the requirements and initial value points. All launch vehicles studied in this project showed similar requirements from the available data but the Falcon 9 would be the best launch vehicle given the dimensions of the satellite.

The biggest limitation of this project was Ansys doesn't have the full capabilities to fully model all structural vibration requirements. When conducting a project of this scale all aspects need to be analyzed to ensure safety and a successful launch. Ansys has no form of acoustic vibration simulation. The acoustics during launch affect the entire structure of the payload, performing the acoustic test is pivotal to obtain the appropriate data. Although Ansys can model some of the structural vibrations, most satellites are run through a series of tests at various labs, where the equipment simulates a launch. To avoid these limitations further testing would need to be performed to accurately predict all vibrations within the structure of the monoblock satellite. Going forward the project would need to identify the limitations and define the desired mission of the satellite. The satellite used was a baseline model and the numbers used for the simulation (payload mass, frequency, etc.) were taken from the launcher requirements. The exact numbers would need to be determined to accurately produce the structural vibration data. Once the satellite was built and the dimensions were determined the testing could be conducted at any of the lab sites. Numerous tests would need to be performed to limit the errors and better model the functionality of the mission. Overall, the future work would align with the scope of this project but would have more accurate numbers. The simulations would follow the same pattern, but would include the acoustic vibrational requirements and a more in depth sinusoidal analysis.

References

- [1] Bhat, B. N., *Aerospace materials and applications*, Reston, VA: American Institute of Aeronautics and Astronautics, 2018.
- [2] Lee, J.-R., and Dhital, D., “Review of flaws and damages in space launch vehicle: Structures,” *Journal of Intelligent Material Systems and Structures*, vol. 24, 2012, pp. 4–20.
- [3] Guzman, L. A., Payload Fairing Geometries as Space Stations with Flexible “Plug and Play” Rack System, 49th International Conference on Environmental Systems, Houston, TX: SICSA, 2019, pp. 113–130.
- [4] Baker, D., *Rockets and launch vehicles: exploring space*, New York: Weigl Publishers, 2009.
- [5] “Components of a Space Launch System,” *Space Foundation*, 2021. Available: https://www.spacefoundation.org/space_brief/components-of-a-space-launch-system/
- [6] Dunbar, B., “Liquid Hydrogen--the Fuel of Choice for Space Exploration,” *NASA*, 2018. Available: https://www.nasa.gov/topics/technology/hydrogen/hydrogen_fuel_of_choice.html
- [7] Baalke, R., “STARDUST Launch Vehicle,” *NASA*, 2000. Available: <https://solarsystem.nasa.gov/stardust/spacecraft/sd-launch.html>
- [8] Dunn, Barrie. D., *Materials and processes: for spacecraft and high reliability applications*, Springer International PU, 2018.
- [9] “Aluminum applications – Transport,” – *Transport*, 2020. Available: <https://www.aluminiumleader.com/application/transport/>
- [10] Braeunig, R. A., *Basics of Space Flight: Rocket Propellants*, 2008. Available: <http://www.braeunig.us/space/propel.html>
- [11] Nassar, L. A., Bonifant, R et al., “Spacecraft Structures and Launch Vehicles,” Virginia Tech, November 2004.
- [12] “Faulty Materials Caused Two Launch Failures: NASA,” *Occupational Health & Safety*, 2019. Available: <https://ohsonline.com/Articles/2019/05/02/Faulty-Materials-Caused-Two-Launch-Failures-NASA.aspx>
- [13] Murty, S. V. S. N., *Case studies in engineering failure analysis*, Elsevier, 2015, pp. 1–9.
- [14] Chiku, N., *Development of Payload Fairings for Launch Vehicle*, Aerospace Systems Company, October 2018.
- [15] “Composite Payload Fairing: Aerospace,” *Composites One*, 2021. Available: <https://www.compositesone.com/benefits-offered-by-composite-rocket-payload-fairings/>. Accessed 6/25/21]
- [16] “ESA and industry collaborate to improve rocket fairings,” *ESA*, 2017. Available: https://www.esa.int/Enabling_Support/Space_Transportation/Ariane/ESA_and_industry_collaborate_to_improve_rocket_fairings
- [17] Jang, J. W., and Alaniz, A., “Design of Launch Vehicle Flight Control Systems Using Ascent Vehicle Stability Analysis Tool,” NASA CR-0523, May 2018.
- [18] Newlands, R. and Heywood, M et al., “Rocket Vehicle Loads and Airframe Design,” *Aspire Space*, January 2016. Available: <http://www.aspirespace.org.uk/downloads/Rocket%20vehicle%20loads%20and%20airframe%20design.pdf>
- [19] Anderson, W. G., Launch Vehicle Avionics Passive Thermal Management, 44th International Conference on Environmental Systems, Lancaster, PA: Advanced Cooling Technologies , 2014, pp. 262–274.

- [20] Kern, L. D., and Scharton, D. T., "NASA Handbook for spacecraft structural dynamics testing," June 2006.
- [21] "Falcon 9 Launch Guide" *SpaceX*, United States, 2009.
[<https://www.spaceflightnow.com/falcon9/001/f9guide.pdf>. Accessed 7/1/21.]
- [22] Wilkins, M., "Atlas V User Guide" *United Launch Alliance*, United States, March 2010.
[<https://www.ulalaunch.com/docs/default-source/rockets/atlasvusersguide2010.pdf>. Accessed 7/1/21.]
- [23] "Delta IV User Guide" *United Launch Alliance*, United States, June 2013.
[<https://www.ulalaunch.com/docs/default-source/rockets/delta-iv-user%27s-guide.pdf>. Accessed 7/2/21.]
- [24] Ellenthorpe, J., "Zenit User Guide" *Land Launch*, Russia, July 2004.
[<http://www.georing.biz/usefull/LLUG.pdf>. Accessed 7/2/21.]
- [25] Perez, E., "Vega User Guide" *ArianeSpace*, France, April 2014.
[https://www.arianespace.com/wp-content/uploads/2018/05/Vega-Users-Manual_Issue-04_April-2014.pdf. Accessed 7/5/21.]
- [26] Laiger, R., "Ariane 5 User Guide" *ArianeSpace*, France, March 2013.
[https://www.arianespace.com/wp-content/uploads/2011/07/Ariane5_Users-Manual_October2016.pdf. Accessed 7/5/21.]
- [27] Zheng, C., and Lei, S., "LM-3A Series Launch Vehicle User Guide," China Great Wall Industry Corporation, China, October 2011.
[<http://www.cgwic.com/launchservices/Download/manual/LM-3A%20Series%20Launch%20Vehicles%20User%27s%20Manual%20Issue%202011.pdf>. Accessed 7/6/21.]
- [28] Inman, D. J., *Engineering vibration*, Estados Unidos: Pearson Education, Inc., 2008.
- [29] DES, A., "Sinusoidal vibration Basics," *Delserro Engineering Solutions* Available:
<https://www.desolutions.com/blog/2014/09/sinusoidal-vibration-basics/>
- [30] "What is fea: Finite element analysis? Documentation," *SimScale* Available:
<https://www.simscale.com/docs/simwiki/fea-finite-element-analysis/what-is-fea-finite-element-analysis/>
- [31] "Falcon Users Guide - SpaceX" Available:
https://www.spacex.com/media/falcon_users_guide_042020.pdf.